

# **ATOMIC-FORCE MICROSCOPY OF CORROSION PITS AND CRACK INITIATION IN FATIGUE OF METALS**

Y. Nakai, Y. Shimizu, S. Fujiwara and T. Ogawa

Department of Mechanical Engineering, Kobe University,  
1-1, Rokkodai, Nada, Kobe 657-8501, Japan

## **ABSTRACT**

In the present study, corrosion fatigue crack initiation of a 13Cr stainless steel and a high-strength aluminum alloy was investigated by using an atomic force microscope (AFM). The corrosion fatigue tests of 13Cr stainless steel were conducted in distilled water and dilute sodium chloride solution, and it was found that the corrosion fatigue life was affected by the environmental condition. The corrosion fatigue life was found to be shorter for higher concentration of sodium chloride. But no influence of dissolved oxygen was found on the corrosion fatigue life. From the surface observation by AFM, no corrosion pits were observed in 100 ppm sodium chloride solution before crack initiation. They formed after crack initiation. In 500 ppm solution, corrosion fatigue cracks were found to be initiated from surface inclusions. In this solution, corrosion pits were also found at the crack initiation site. The sizes of the pits just after initiation were almost independent of the concentration of sodium chloride. The growth rates of the pits, however, were higher for higher concentration of the solution. The fatigue strength of 7075-T651 alloy in 3% NaCl solution was also much lower than that in air. In this material, corrosion pits were observed prior to crack initiation, and corrosion fatigue cracks were found to be initiated either at corrosion pits or grain boundaries. For crack initiation at corrosion pits, it was not nucleated from the deepest point of the pit. The crack initiation site within the pit was also the grain boundary.

## **KEYWORDS**

Corrosion fatigue, Corrosion pit, AFM, Stainless steel, High strength aluminum alloy

## **INTRODUCTION**

Since microscopic observation is the most useful method to clarify the mechanisms of fatigue processes in materials, the progress of metal fatigue study has strongly depended on the development of new microscopic observation methods such as optical microscopy (OM), transmission electron microscopy (TEM), and scanning electron microscopy (SEM). Recently, we obtained a new microscope called as "Scanning Probe Microscope (SPM)", which gives us three-dimensional images of solid surfaces on the atomic scale. It has excellent capabilities for analyzing the topographic nature of solid surfaces. Recently, many types of the scanning probe have been developed. Among SPMs, scanning tunneling microscope (STM) and scanning atomic force microscope (AFM) are now widely employed for the studies of strength of materials because the surface morphology of materials can be observed with atomic scale resolution with these microscopes. By using STM

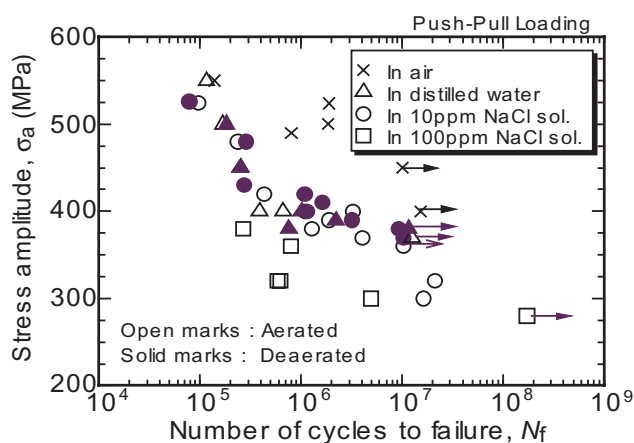
and AFM, Komai and others [1] observed the micro-crack initiation and growth behavior in stress corrosion cracking. Matsuoka and others observed cleavage fracture surface [2]. For fatigue micro-mechanisms, Ishii and others [3] observed fatigue slip band with STM. They also examined fatigue striation shape with AFM [4]. Yoon and others observed nucleation mechanism of intergranular cracks in high-cycle fatigue [5]. Ohgi and others observed crack initiation at grain boundary in low-cycle fatigue [6]. Nakai and his co-workers have been studied on fatigue slip bands, fatigue crack initiation, and the growth behavior of micro-cracks in a structural steel [7] and  $\alpha$ -brass [8]-[12]. Nakai and Oida [13], Saxena and others [14], and Ogawa and Hatanaka [15] observed the change of surface roughness during fatigue test in air. Nakai and Shimizu studied corrosion pits and crack initiation mechanisms in corrosion fatigue of a stainless steel [16].

In the present paper, corrosion fatigue tests of 13Cr stainless steel and high strength aluminum alloy were conducted in sodium chloride solutions, and crack initiation mechanisms were observed by means of optical microscopy and scanning atomic force microscopy (AFM) to clarify corrosion fatigue crack initiation mechanisms.

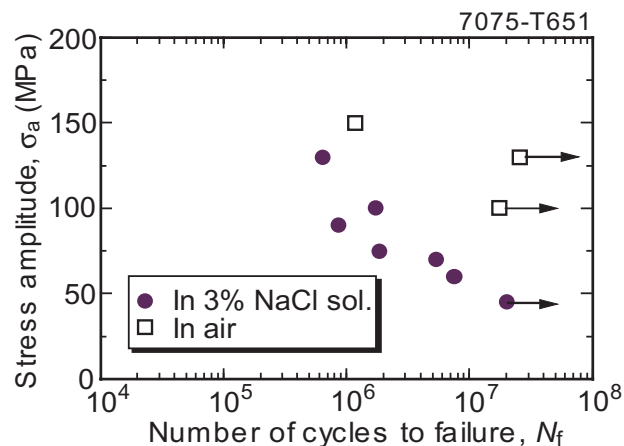
## EXPERIMENTAL PROCEDURE

The material for the present study was a 13Cr stainless steel, AISI 414, and a high strength aluminum alloy, 7075-T651. The chemical composition, mechanical properties, and heat treatment conditions of the materials were described elsewhere [16, 17]. Prior to the fatigue tests, the surface of specimens was polished by buffing. The specimen has a minimum cross section of width 8 mm and thickness 4 mm, and has weak stress concentration with the elastic stress concentration factor 1.03 under plane bending and 1.13 under push-pull loading [16]. The push-pull loading fatigue tests were carried out in a computer controlled electro-hydraulic fatigue testing machine, and a computer controlled electro-dynamic vibrator was employed for the plane-bending fatigue tests. They were operated at a frequency of 30 Hz under fully reversed cyclic loading ( $R = -1$ ).

Since it was very difficult to identify in advance where fatigue cracks would be nucleated, we took replicas at the predetermined numbers of fatigue cycles. The replica films were coated by Au before observations. Although the height of the surface is reversed from the original surface by the replication method, the height of the replica film in the AFM images was reversed by an image processing technique. An scanning probe microscope (Seiko Instruments Inc.: SPA-350), which has large stage unit, was employed for the present AFM observation. The resolution of the microscope is 0.5 nm in the surface direction and 0.1 nm in the vertical direction. The region for AFM observation was determined by optical microscopy at a magnification of 2000 on a CRT monitor. In the present study, corrosion fatigue tests of the stainless steel were conducted in sodium chloride aqueous solution from 0 to 500 ppm, and the effect of sodium chloride concentration and dissolved oxygen on the corrosion fatigue life and crack initiation mechanism were examined. The corrosion fatigue tests of the aluminum alloy were conducted in 3% sodium chloride aqueous solution.



(a) 13Cr stainless steel (Push-pull loading).



(b) High-strength aluminum alloy (Plane bending).

Figure 1: S-N curves.

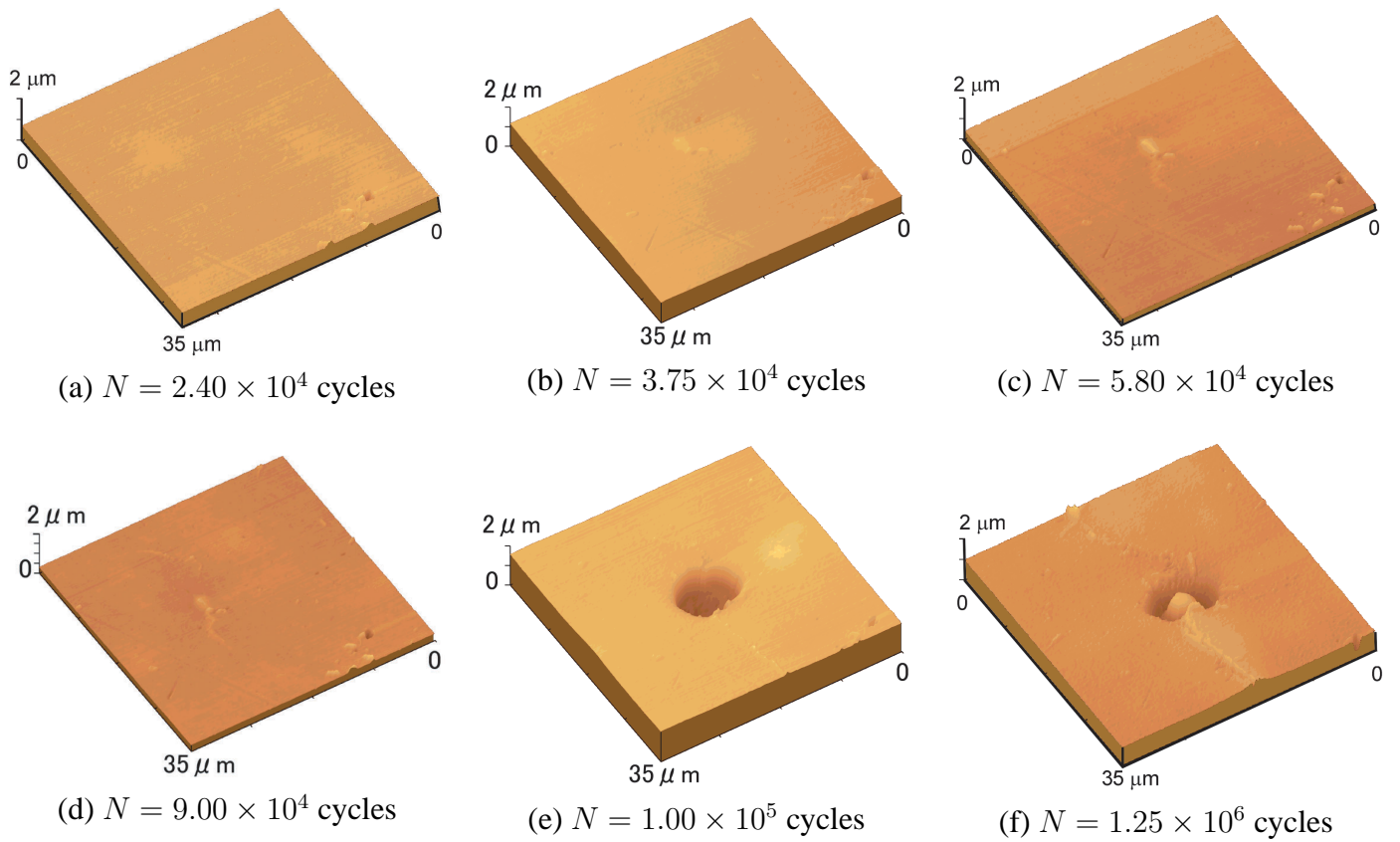


**Figure 2:** AFM images of surfaces in 100 ppm NaCl solution at  $\sigma_a = 430$  MPa (13Cr stainless steel, Scanning area:  $35 \mu\text{m} \times 35 \mu\text{m}$ ).

## EXPERIMENTAL RESULTS

### *S-N Curves*

Figure 1 shows the relation between stress amplitude,  $\sigma_a$ , and number of cycles to failure,  $N_f$ . In either material, the fatigue life in aqueous environments was shorter than that in air. In 13Cr stainless steel, the fatigue life in 10 ppm NaCl solution was almost the same for that in distilled water. The fatigue life in 100 ppm NaCl solution, however, was shorter than that either in 10 ppm solution or in distilled water. For either concentration of NaCl solution, the fatigue life in aerated solution was almost the same for that in deaerated solution. In push-pull loading, some cracks were initiated from the cylindrically curved side surface. Since it was easier to make observation on the plane surface than on the curved surface when the magnification of the microscope was high, plane bending fatigue tests were conducted. There were no significant difference in fatigue life between plane bending and push-pull loading [16].

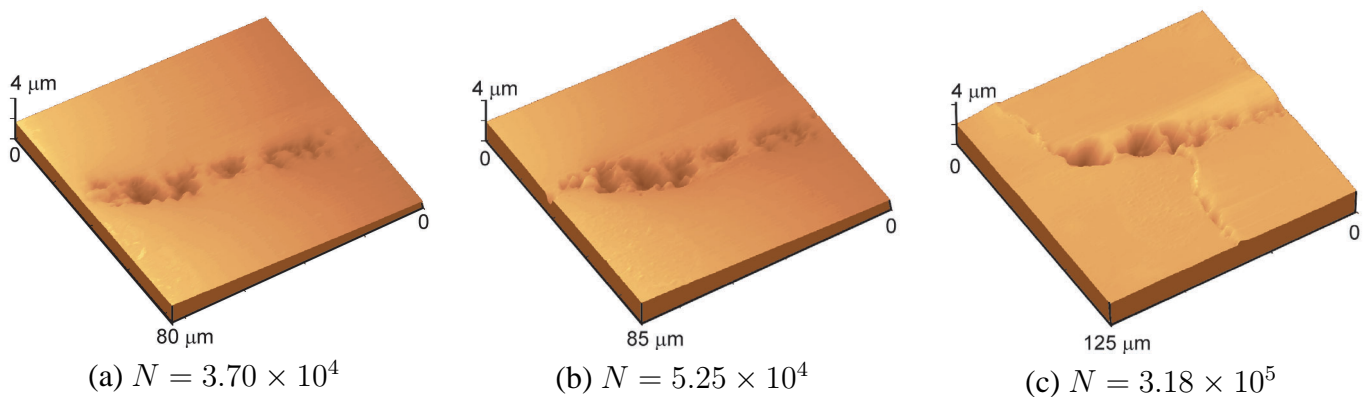


**Figure 3:** AFM images of surfaces in 500 ppm NaCl solution at  $\sigma_a = 430$  MPa (13Cr stainless steel).

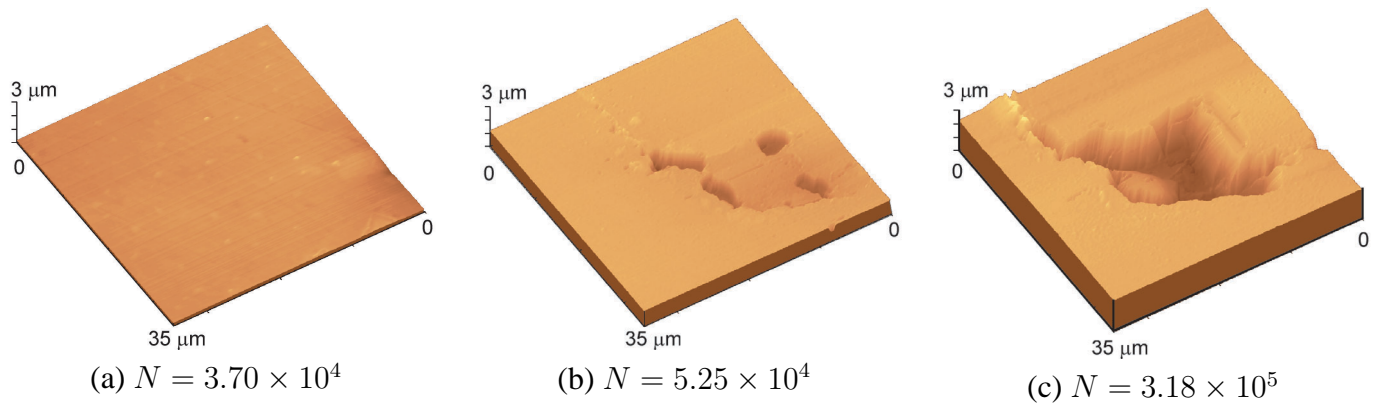


**Figure 4:** Higher magnification AFM images of surfaces in 500 ppm NaCl solution (13Cr stainless steel,  $\sigma_a = 430$  MPa).

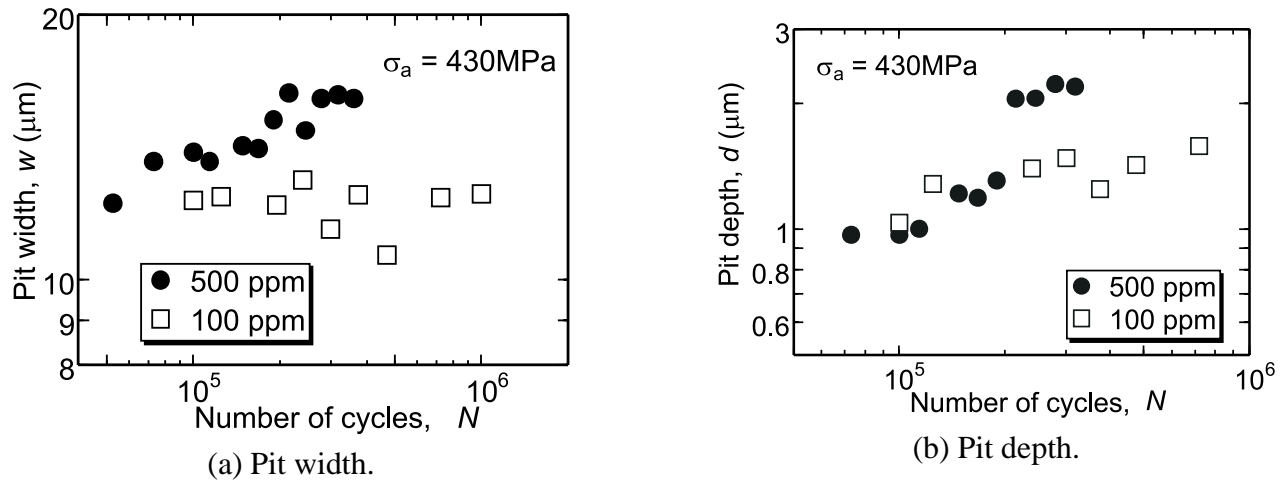


**Figure 5:** Change of pit sizes (13Cr stainless steel).

### 13Cr Stainless Steel

#### Crack initiation process

Either in distilled water and in 10 ppm sodium chloride solution, no cracks were initiated from corrosion pits, then the mechanism of crack initiation in these solutions may be similar to that in air.

AFM images of the specimen surface fatigued in 100 ppm solution are shown in Fig. 2. In these figures, extrusions are found in (b) ( $N = 3.75 \times 10^4$ ), and a crack was initiated from the extrusions in (c) ( $N = 5.80 \times 10^4$ ). The extrusion is considered to be corrosion product, which was formed at bare metal surface produced by a crack embryo. A corrosion pit was formed at the crack initiation site in (e) ( $N = 1.00 \times 10^5$ ). Then, it is evident from the AFM observation that the fatigue crack was initiated before the corrosion pit appeared, and a corrosion pit was found to be initiated along the crack, while optical micrographs showed that a crack was initiated from the corrosion pit. Therefore, it is important to notice that we sometimes misunderstand the corrosion fatigue crack initiation process from optical microscopy.

Figures 3 and 4 are AFM images of the corrosion fatigue process in 500 ppm sodium chloride solution at  $\sigma_a = 430$  MPa, where images in Fig. 4 are higher magnification images of the crack initiation site of the inclusion. In this case, corrosion pits were appeared almost at the same time of the crack initiation. These results were consistent with those with optical microscopy. Inclusions also existed in specimens those were fatigued in 10 ppm solution, 100 NaCl solution, and in distilled water, but they were not crack initiation site in these environments.

#### Growth behavior of corrosion pits

Depth and surface width of a corrosion pit can be measured from cross-section geometry of the pits, which

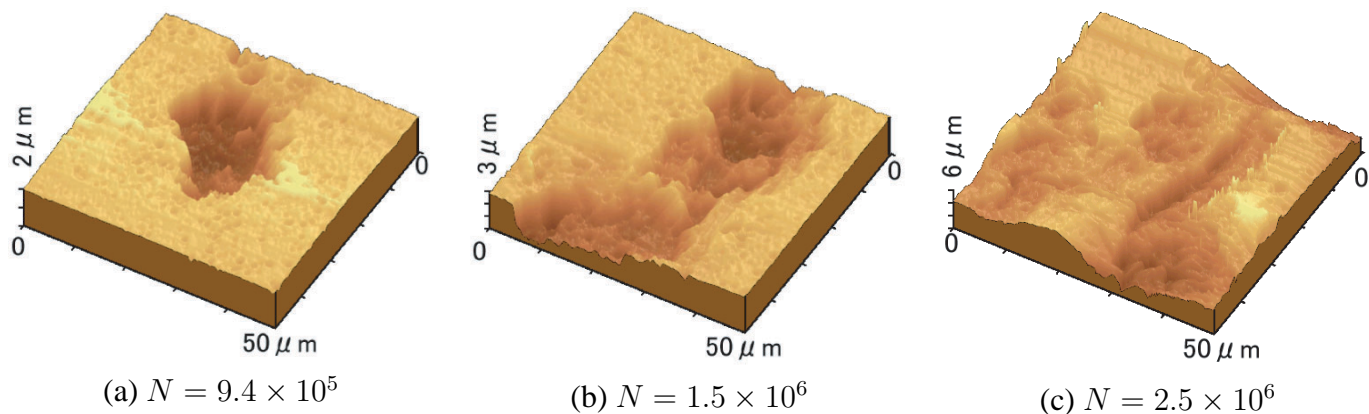


**Figure 6:** AFM images of crack initiation from corrosion pit (High-strength aluminum alloy).

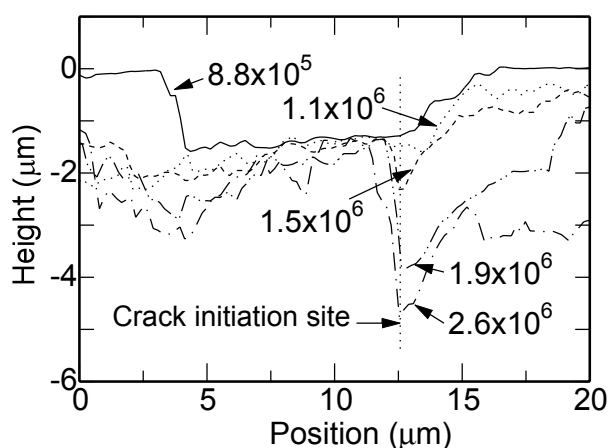


**Figure 7:** Change of geometry of a corrosion pit (High-strength aluminum alloy).

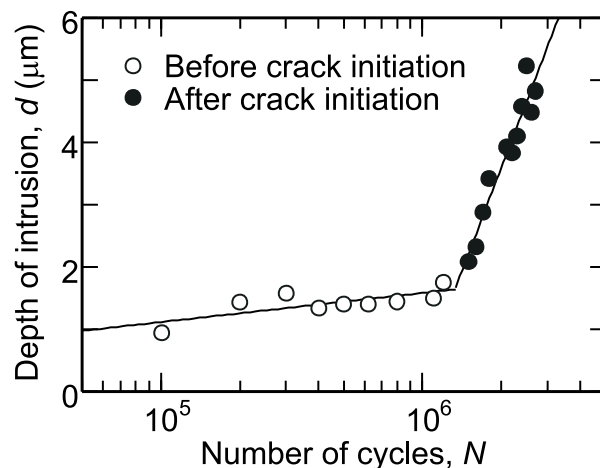


**Figure 8:** Change of intrusion depth in fatigue process (High-strength aluminum alloy).

can be obtained from AFM image. Changes in the size of corrosion pits are plotted as a function of number of cycles in Fig. 5, where the pit width was measured perpendicular to the loading direction. The stress amplitude for these observations was 430 MPa, and the concentration of NaCl was either 100 ppm or 500 ppm. Although the sizes of corrosion pits just after initiation was almost independent of the concentration of NaCl, the growth rate of the pits was higher for higher concentration of NaCl. The aspect ratio of corrosion pit was almost independent of the concentration of NaCl, and it gradually increased with number of cycles. The aspect ratio, however, remained 0.14 at the final stage of corrosion fatigue, then, the stress concentration by these pits were small.

### **High Strength Aluminum Alloy**

AFM images of the specimen surface fatigue at a stress amplitude of 100 MPa were shown in Fig. 6, where arrows indicate the loading direction. The corrosion pit was initiated at very early stage of fatigue process, and it grew with number of cycles, and a crack was initiated from the pit. The crack initiation at  $N = 1.5 \times 10^6$  could be identified clearly from AFM images. The change of the geometry of cross-section is indicated in Fig. 7. No cracks were initiated from the deepest point of the corrosion pit. It was initiated at a grain-boundary within the pit. As shown in Fig. 8, the growth rate of the intrusion depth at crack initiation site was accelerated with crack initiation.

Even for a crack whose optical micrographs showed that it was initiated from grain-boundary without corrosion pit, AFM images sometimes indicated that there was a small pit at the crack initiation site. In that case it was not clear whether the pit was nucleated after or before crack initiation [18].

## **CONCLUSIONS**

Corrosion fatigue tests of a 13Cr stainless steel and a high strength aluminum alloy were conducted in sodium chloride solutions, and the initiation processes of cracks and corrosion pits were observed by means of optical microscopy and scanning atomic-force microscopy. The following results were obtained:

(1) In both materials, the fatigue life in aqueous environment was shorter than that in air. In the stainless steel, the corrosion fatigue life was shorter for higher concentration of sodium chloride. But no influence of dissolved oxygen was found on the corrosion fatigue life.

(2) In the stainless steel, no cracks were initiated at corrosion pits when the concentration of sodium chloride was less than 10 ppm. In 500 ppm solution, cracks were found to be initiated from surface inclusions. In this solution, corrosion pits were also found at the crack initiation site.

(3) In the aluminum alloy, cracks were initiated either at corrosion pits or grain boundaries. For crack initiation at corrosion pits, it was not nucleated from the deepest point of the pit. The crack initiation site within the pit was also the grain boundary.

## REFERENCES

1. Komai, K., Minoshima, K., and Itoh, M. (1994). *J. Soc. Mat. Sci., Japan*, 43, 336.
2. Matsuoka, S., Sumiyoshi, H., and Ishikawa, K. (1990). *Trans. Japan Soc. Mech. Eng.*, 56A, 2091.
3. Ishii, H., Yamanaka, S., and Tohgo, K. (1995). In: *ICM 7 (Proc. 7th Int. Conf. Mech. Behav. Mat.)*, pp.367-368, ESIS.
4. Choi, S., Ishii, H., and Tohgo, K. (1998) *J. Mat. Sci., Japan*, 47, 852.
5. Yoon, W. K., Inoue, T., Noguchi, H., and Higashida, K. (1998). *Trans. Japan Soc. Mech. Eng.*, 64A, 1435.
6. Ohgi, J., Hatanaka, K., and Zenge, T. (1998). In: *Experimental Mechanics, Advances in Design, Testing and Analysis*, pp.1053-1058, Allison I. M. (Ed), Balkema, Rotterdam.
7. Nakai, Y., Fukuhara, S., and Ohnishi, K. (1997). *Int. J. Fatigue*, 19S., 223.
8. Nakai, Y., Ohnishi, K., and Kusukawa, T. (1999). *Trans. Japan Soc. Mech. Eng.*, 65A, 483.
9. Nakai, Y., Ohnishi, K., and Kusukawa, T. (1999). In: *Small Fatigue Cracks: Mechanics and Mechanisms*, pp. 343-352, Ravichandran, K. S., Ritchie, R. O., and Murakami, Y. (Eds), Elsevier, Oxford.
10. Nakai, Y., Kusukawa, T. and Hayashi, N. (1999). *ATEM'99 (Proc. Int. Conf. Adv. Tech. in Exp. Mech.)*, Vol. 1, pp.152-157, Jpn Soc. Mech. Eng.
11. Nakai, Y. and Kusukawa, T. (2001). *Trans. Jpn Soc. Mech. Eng.*, 67A, 476.
12. Nakai, Y., Kusukawa, T., and Hayashi, N. (2001). In: *ASTM STP* (To be published).
13. Nakai, Y. and Oida, M. (1999). In: *Fatigue '99 (Proc. 7th Int. Fatigue Conf.)*, pp.2771-2776, EMAS, West Midlands, U.K..
14. Saxena, A., Yang, F., and Cretegnny, L. (1999). *Fatigue '99 (Proc. 7th Int. Fatigue Conf.)*, pp.2777-2782, EMAS, West Midlands, U.K..
15. Ogawa, H. and Hatanaka, K. (1999). In: *ATEM'99 (Proc. Int. Conf. Adv. Tech. in Exp. Mech.)*, Vol. 1, pp.158-161, Jpn Soc. Mech. Eng.
16. Y. Nakai, Y. Shimizu, and N. Saeki (1999). In: *ICM8 (Progress in Mechanical Behavior of Materials)*, Vol. I, pp.364-369, Ellyin, F. and Provan, J. W. (Eds).
17. Nakai, Y., Kondo, K., and Ohji, K. (1992). *Trans. Jpn Soc. Mech. Eng.*, 58A, 359.
18. Nakai, Y., Fujiwara, S., Ogawa, T., and Shimizu, Y. (2001). *Materials Science Research International, STP-1*, 101.